Time-Resolved Light Scattering Studies on the Kinetics of Phase Separation and Phase Dissolution of Polymer Blends. 2. Phase Separation of Ternary Mixtures of Polymer A, Polymer B, and Solvent†

Takeji Hashimoto,* Kouji Sasaki,‡ and Hiromichi Kawai§

Department of Polymer Chemistry, Faculty of Engineering, Kyoto University, Kyoto 606, Japan. *Received December 19, 1983*

ABSTRACT: The mechanism and kinetics of the phase separation of ternary mixtures of PS/PB/Tol and PS/SB/Tol [PS, PB, SB, and Tol represent respectively polystyrene, polybutadiene, polystyrene–polybutadiene diblock polymer, and toluene (a good solvent for each of these polymers)] were studied by the time-resolved light scattering technique. In this method, evolution of the structure with time after the temperature drops from temperatures above the cloud points to those below them was isothermally observed at given polymer concentrations as a function of quench depth, ΔT, and polymer compositions. It was found that (i) an early stage of spinodal decomposition (up to a few tens of seconds for the particular systems studied) can be described by the linearized theory proposed by Cahn and that (ii) the time-dependent variation of the scattering profiles dramatically depends on the phase-separation mechanism (spinodal decomposition vs. nucleation and growth). It was also found that (iii) the phase-separated structures observed in solvent-cast films are generally those which were frozen in at some concentrations during the solvent evaporation process and very much reflect the spinodal decomposition and its coalescence processes occurring in the solutions.

I. Introduction

Previously we presented results on the kinetics of phase separation of binary mixtures of polystyrene (PS) and poly(vinyl methyl ether) (PVME).[1] Here we extend the studies[17,26-28] to ternary mixtures of PS/PB/Tol and PS/SB/Tol, where PB, SB, and Tol denote, respectively, polybutadiene, PS–PB diblock polymer, and toluene, a good solvent for both PS and PB. It is our primary objective in these studies to investigate the mechanism and kinetics of phase separation of the ternary system rather than to investigate quantitatively the phase equilibrium of such systems, although the latter problem itself is of current interest to many researchers, and we also will present cloud-point curves (section III-2).

In this paper we present the time-resolved light scattering apparatus used in these studies (section II-2), morphology and light scattering patterns of the films prepared by casting toluene solutions on mixtures of PS/PB, PS/SB, and PS/SB/PB (section III-1), cloud-point curves of ternary systems of PS/PB/Tol and PS/SB/Tol (section III-2), and time-resolved light scattering data (section III-3). From the results obtained in sections III-1 and III-3, it will be shown that the phase-separated structure observed in solvent-cast films is strongly affected by the structure existing in the solutions. Periodic concentration fluctuations of PS and PB or PS and SB which are formed in solution by spinodal decomposition and its following coalescence processes tend to be frozen in at some concentration levels resulting in the structure in the solid state. In section III-3 is presented qualitatively experimental evidence supporting Cahn's linearized theory of spinodal decomposition in the ternary systems. The present paper may be regarded as an extension of the studies reported by Van Aartsen et al.[21-23] on the spinodal decomposition of polymer–solvent binary systems.

† Presented in part at the 30th Annual Meeting, Society of Polymer Science, Japan, May 1981, Kyoto, Japan (*Polym. Prepr., Jpn* **1981** 30 (3), 483), and at the 30th Polymer Symposium, Society of Polymer Science, Japan, Oct 1981, Tokyo, Japan (*Polym. Prepr., Jpn.* **1981**, *30* (9), 2098).

‡ Present address: Toyoda Gosei Co., Ltd., 1, Nagahata, Ochiai, Haruhi-mura, Nishikasugai-Gun, Aichi-Prefecture 452, Japan.

§ Present address: Hyogo University of Education, Yashiro-cho, Kato-Gun, Hyogo-ken 673-14, Japan.

Table I
Characterization of Sample

	$10^{-3}M_n$[a]	M_w/M_n[b]	density,[c] g/cm^3	microstructure,[d] wt %: cis-1,4	trans-1,4	1,2-, 3,4-linkages
PS	151	1.41	1.053			
PB	48	1.23	0.895	46	45	9
SB	50	1.7	0.952	35	52	13

[a] Measured by membrane osmometry. [b] Measured by GPC. [c] From "Polymer Handbook". [d] Measured by IR spectroscopy.

II. Experimental Methods

Polymers PS, PB, and SB were prepared by living anionic polymerization in a nitrogen atmosphere. They have characteristics as shown in Table I.

Polymer films composed of binary mixtures of PS and PB (designated as S/B) or PS and SB (designated as S/SB) and ternary mixtures of PS, PB, and SB (designated as S/B/SB) were prepared by pouring toluene solutions onto a glass plate at room temperature. Toluene was evaporated at the natural rate, and it took about 3–5 min before thin solid films were obtained. Total polymer concentration was kept initially at 10% by weight. The phase-separated structures were observed by phase-contrast optical microscopy with the films unstained or stained by OsO_4 and by a laser light scattering photometer briefly described in a previous paper.[1]

In order to measure cloud points, a given ternary mixture was sealed in a glass tube to keep the concentration constant. Cloud points were measured by lowering the temperature from temperatures well above the cloud points and by observing visually macroscopic phase separation between the two polymer solutions (e.g., PS solution and PB (or SB) solution). The system was kept at constant temperature at least for 15 min in order to judge if the system undergoes phase separation at that temperature. The cloud points were estimated with accuracy to ±1 °C.

Figure 1 shows the laser light scattering apparatus used in the studies in order to record change of the scattering profiles with time during phase separation. A plane-polarized laser beam (He–Ne laser of 20 mW, λ_0 = 6328 Å) was used as an incident source. The polarization direction of the beam can be rotated by a polarization rotator (its essential part being one-half-wavelength retardation plate). The 10-mm diameter, 1-mm thick sample cell was made of quartz and was placed in a temperature enclosure mounted on a horizontal xy stage. The scattered light intensity was recorded through an analyzer onto Polaroid Land Pack films or by a TV camera system composed of a silicone

0024-9297/84/2217-2812$01.50/0

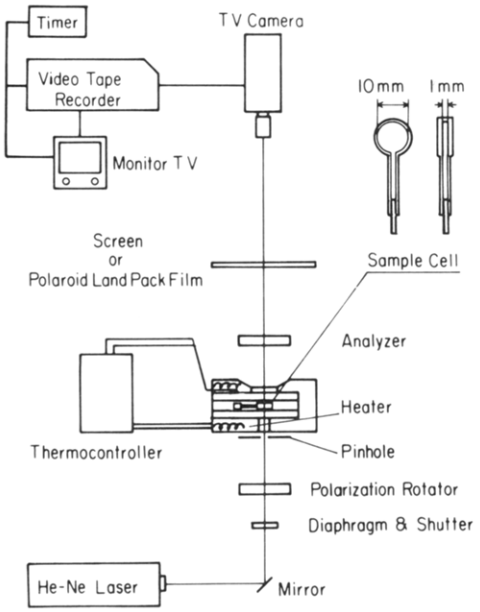

Figure 1. Schematic diagram showing a time-resolved light scattering apparatus used in this work.

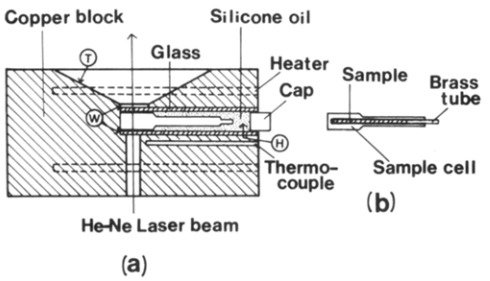

Figure 2. Sample cell to enclose polymer solution and a heated metal block controlled at phase-separation temperature T_x to which the sample cell is inserted rapidly and manually for the temperature-drop experiments.

vidicona, video tape recorder (VTR), and a TV monitor capable of recording 60 frames/s. A timer is triggered synchronously with insertion of the sample cell into the temperature enclosure, and the time after the insertion was recorded on the VTR and displayed on the TV monitor.

Figure 2 represents a schematic disagram of the temperature enclosure. The entrance of the sample cell was fused with a brass tube, whose end was soldered after enclosure of the solution to avoid solvent leakage (Figure 2b). The ternary solution enclosed in the cell was placed in a silicone oil bath whose temperature was regulated at 50 °C, above the cloud points. The sample cell was then rapidly and manually transferred into a heated copper block regulated at a phase-separation temperature T_x below the cloud points (Figure 2a). The copper block has a hole H in which the sample cell was inserted and held firmly. The windows for the incident and scattered light beam W were sealed by cover glasses, and the hole was filled with silicone oil. The silicone oil has a refractive index close to the cover glasses and quartz cell, thus reducing the reflectivity of light. It also enhances heat conduction between the sample cell and the heated copper block, thus reducing the time required for the temperature drop. The copper block has a tapered window T to detect the scattered light over large scattering angles. The rate of temperature drops from 50 °C to T_x (as low as 30 °C) was measured by inserting a thermocouple in the sample cell filled with toluene and was characterized by a single relaxation time of 9.8 s.

III. Results and Discussion

1. Phase-Separated Structure in Solvent-Cast Films. Figures 3 and 4 represent typical light scattering patterns (V_V scattering) from the thin films prepared by casting from toluene solutions and corresponding optical

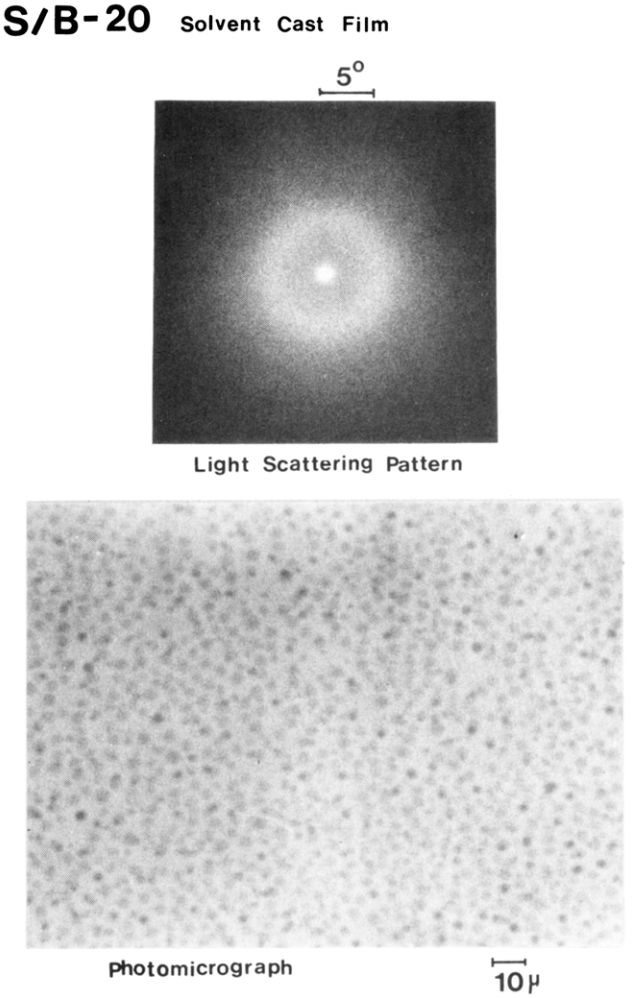

Figure 3. Light scattering pattern and photomicrograph of the solvent-cast film of S/B-20 stained by OsO_4. Toluene is used as a solvent.

micrographs taken with the films stained by OsO_4 vapor for S/B-20 containing 20 wt % PB and S/SB-65 containing 65 wt % SB. The dark dispersed domains in Figure 3 and the matrix in Figure 4 should be the PB-rich domains and SB-rich matrix stained by OsO_4, respectively. The bright phase, on the other hand, should correspond to the unstained PS-rich phase. It is most interesting to note that the phase-separated structure clearly exhibits the scattering maximum as shown in these figures. It must be a fundamental problem, associated with mechanism of structural evolution during phase separation induced by solvent evaporation, to answer whether the maximum arises from *interparticle interference* or *intraparticle interference*. If it arises from the interparticle interference, the maximum reflects regularity in the interparticle distance, while if it arises from the intraparticle interference it reflects uniformity of the particle size.

A similar scattering maximum was reported also by Dupplessix, Picot, and Benoit[3] for the solvent cast films of the ternary polymer blends of PS, poly(methyl methacrylate) (PMMA), and PS–PMMA diblock polymers. They attributed the scattering maximum to the intraparticle interference maximum and estimated mean particle size and its standard deviation. A fundamental question arises naturally on what is the physical driving force which leads to the particle size being uniform so as to give the intraparticle interference maximum. This question motivated the studies in the present and forthcoming papers.

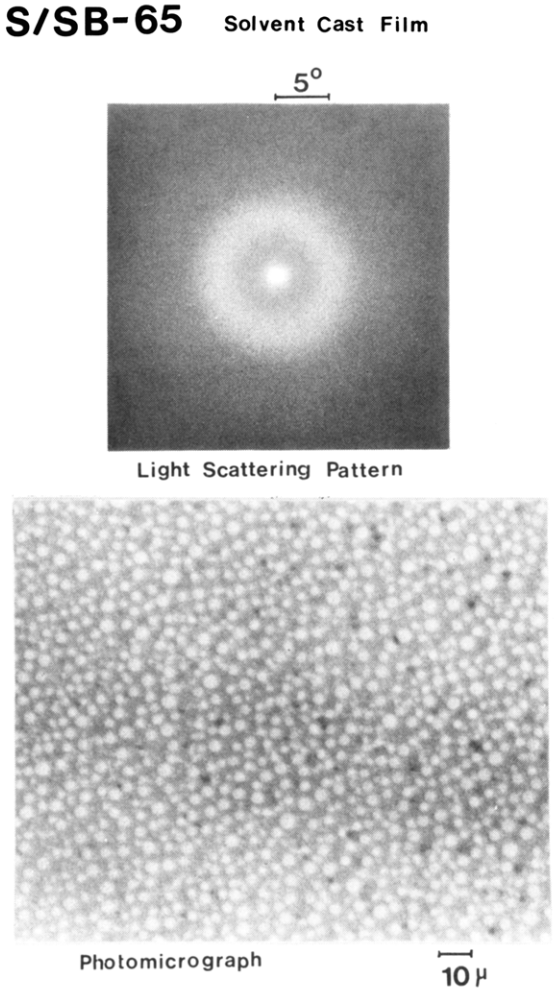

Figure 4. Light scattering pattern and photomicrograph of the solvent-cast film of S/SB-65 stained by OsO_4. Toluene is used as a solvent.

In order to clarify the origin of the scattering maximum, we prepared a series of thin films composed of the binary and ternary mixtures by casting their toluene solutions (total polymer concentrations being 10 wt %) onto a glass plate. The binary and ternary mixtures of PS, PB, and SB studied here have the following chemical compositions as denoted by S/B/SB in wt %: 20/80/0, 80/20/0, 35/0/65, 65/0/35, 66/2/32, 70/9/21, and 73/16/11. All these mixtures show the scattering maximum as shown typically in Figures 3 and 4. An image analysis of these optical micrographs gave the average radius of the dispersed domains R_m and interdomain distance D_m.

The size of the domains and the interdomain distance were also estimated by the light scattering maximum. With an assumption that the maximum arises from intradomain interference, the average radius of the dispersed domain R_s may be estimated from[29]

$$4\pi(R_s/\lambda) \sin(\theta_m/2) = 5.765 \quad (1)$$

where θ_m is the scattering angle where the intensity becomes maximum, and λ is the wavelength of light in the medium. With an assumption that the maximum arises from interparticle interference, the average interdomain distance D_s may be estimated from[30]

$$2D_s \sin(\theta_m/2) = \lambda \quad (2)$$

The structural parameters R_m, D_m, R_s, and D_s thus estimated are summarized in Table II and R_m and D_m are compared with R_s and D_s, respectively, the results being shown in Figures 5 and 6. It is clearly shown that correlation between D_s and D_m is much better than that between R_s and R_m, suggesting that the scattering maximum in our systems arises from regularity in the *interdomain distance* rather than uniformity of the dispersed domain

Table II
Characterization of Solvent-Cast Films of Binary and Ternary Mixtures of PS, PB, and SB

blends	composition,[a] wt % S/B/SB	optical microscopy,[b] μm R_m	D_m	light scattering[c] R_s	D_s
B1	20/80/0	3.0	12.6	12.4	13.6
B2	80/20/0	2.5	6.2	6.5	7.1
B3	35/0/65	2.1	6.2	7.3	8.0
B4	65/0/35	4.8	14.7	14.5	15.8
T1	66/2/32	9.0	26.9	23.8	25.9
T2	70/9/21	2.5	9.6	10.1	11.0
T3	73/16/11	2.2	8.7	9.0	9.8

[a] S/B/SB denotes wt % of PS, PB, and SB in the mixture. [b] R_m and D_m are the average radius of the dispersed domains and interdomain distance as measured by optical microscopy, respectively. [c] R_s and D_s are the average radius of the dispersed domains and interdomain distances as estimated by light scattering maximum, based on eq 1 and 2, respectively.

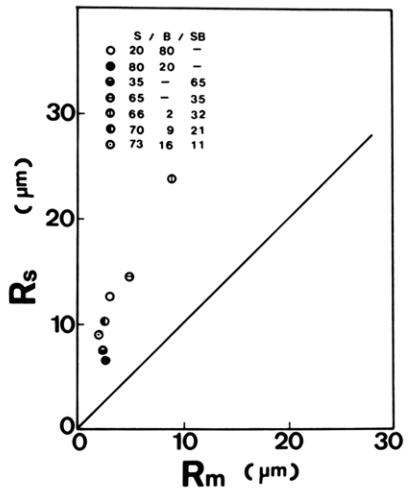

Figure 5. Relation between average radius of the dispersed domain size R_m as measured by photomicroscopy and that R_s as measured by the light scattering pattern by assuming that the scattering maximum arises from intraparticle interference (i.e., eq 1 being used to estimate R_s) for thin film composed of various binary and ternary polymer blends as shown in the figure.

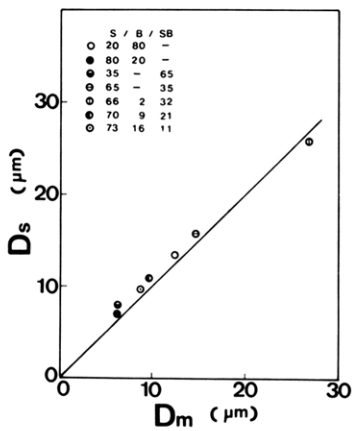

Figure 6. Relation between average interdomain distance D_m as measured by photomicroscopy and that D_s as measured by the light scattering pattern by assuming that light scattering maximum arises from interparticle interference (i.e., eq 2 being used to estimate D_s) for thin films composed of various binary and ternary polymer blends as shown in the figure.

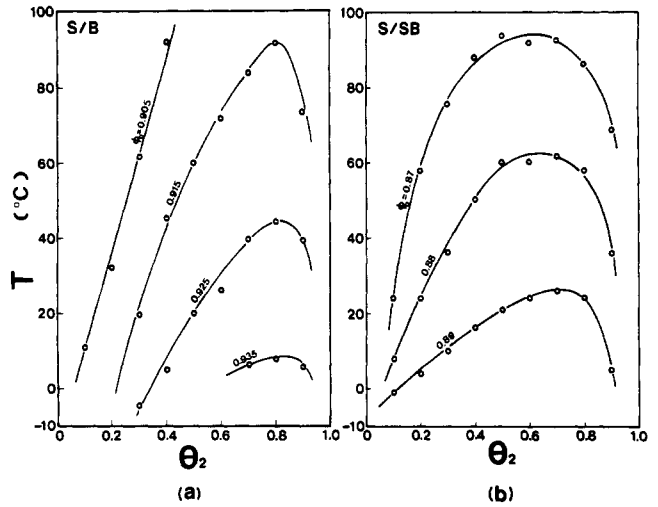

Figure 7. Cloud-point curves for the ternary systems of (a) S/B/Tol and (b) S/SB/Tol at various volume fraction of solvent (toluene) ϕ_0. θ_2 is the volume fraction of polybutadiene or polystyrene–polybutadiene diblock polymer in the polymer mixture.

size, contrary to the case reported by Dupplessix et al.[3]

At this point one can further advance his argument and ask why the interdomain distance is regular to such a level that the regularity gives rise to the scattering maximum. It may be needless to say that the regularity must reflect a very basic aspect of structure formation from the solution, clarification of which is one of the objectives of the present studies and will be discussed in sections III-2 and III-3. During the solvent evaporation process, the concentration of the solution increases, and the phase separation starts to occur and grow according to the mechanism of *nucleation and growth* (*NG*) or *spinodal decomposition* (*SD*). The structure developed in the solution will be *frozen in* at some stage of phase separation where the concentration becomes high and viscosity becomes high, such that the system cannot attain equilibrium with a given time scale of the solvent evaporation process. The frozen-in structure in the solution appears essentially in the structure observed in the solvent-cast films. In order to confirm this speculation, a further experiment was conducted on real-time observation of light scattering profiles during phase separation at given temperatures and polymer concentrations.

2. Cloud-Point Curves. The cloud-point curves for PS/PB/Tol and PS/SB/Tol are shown in parts a and b of Figure 7, respectively, where ϕ_0 is volume fraction of the solvent in the ternary system, and θ_2 is the volume fraction of PB or SB in the polymer mixture. Below the upper critical solution temperature T_c, the solution undergoes phase separation between polystyrene solution and polybutadiene solution (or SB solution). The critical temperature increases with increasing polymer concentration $(1 - \phi_0)$ as shown in Figure 8. For a given polymer concentration, T_c for PS/PB/Tol is much higher than that for PS/SB/Tol, which may be reasonable because the Flory interaction parameter[4] χ_{23} between PS and PB is much larger than that between PS and SB. It should be noted here that T_c in Figure 8 is really the cloud-point maximum. This cloud-point maximum is not necessarily identical with the critical temperature, due to the fact that most polymer blends have asymmetric free energy functions. Nevertheless, we will qualitatively compare the composition of the mixture at which the cloud point becomes maximum with the critical compositions predicted by Scott's mean-field theory. Rigorously speaking, this

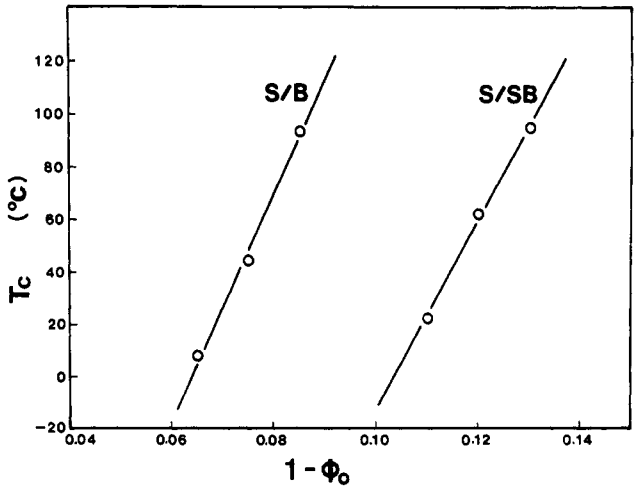

Figure 8. Cloud-point maximum as a function of total polymer concentration $(1 - \phi_0)$ for S/B/Tol and S/SB/Tol.

comparison will not make sense, but it will provide some insights on the measured cloud-point curves.

Mean-field theory predicts[5,6] that the critical composition ($\theta_{1,c}$ and $\theta_{2,c}$) is given by

$$\theta_{1,c} = m_2^{1/2}/(m_1^{1/2} + m_2^{1/2}) \quad (3)$$

$$\theta_{2,c} = m_1^{1/2}/(m_1^{1/2} + m_2^{1/2}) \quad (4)$$

and

$$\chi_{23,c} = (m_1^{-1/2} + m_2^{-1/2})^2/2 \quad (5)$$

where m_1 and m_2 are, respectively, degree of polymerization of PS and PB (or SB) relative to the toluene molecule. Noting that the molecular volumes of toluene, styrene monomer, and butadiene monomer are 106.85, 115, and 98.2 cm^3/mol, respectively, and calculating the monomer molecular volume of SB from the volume-average of the corresponding values of styrene and butadiene, one obtains, m_1 for PS (m_S)

$$m_S = (2.129 \times 10^5)115/(104.15 \times 106.85) = 2.20 \times 10^3$$

and also m_2 for PB (m_B) and for SB (m_{SB})

$$m_B = (5.904 \times 10^4)87/[(54.09)(106.85)] = 8.89 \times 10^2$$

$$m_{SB} = (8.5 \times 10^4)98.2/[(74.11)(106.85)] = 1.05 \times 10^3$$

where weight-average molecular weight was used to calculate the degree of polymerization. The critical composition $\theta_{2,c}$ is then estimated as

$$\theta_{2,c} = 0.61 \quad \text{for PS/PB/Tol} \quad (6)$$

$$\theta_{2,c} = 0.59 \quad \text{for PS/SB/Tol} \quad (7)$$

irrespective of total polymer concentrations $(1 - \theta_0)$. These values predicted by the Scott theory[5] are compared with the experimental values

$$(\theta_{2,c})_{obsd} = 0.80 \quad \text{for PS/PB/Tol} \quad (8)$$

$$(\theta_{2,c})_{obsd} = 0.62 \quad \text{for PS/SB/Tol} \quad (9)$$

Agreement between the experimental and theoretical values is not good for PS/PB/Tol. The experimental values for $\theta_{2,c}$ seem to depend slightly on polymer concentration $1 - \phi_0$, which again is not in good agreement with the theoretical prediction.

3. Time-Resolved Light Scattering Studies. In order to confirm the speculation presented in section III-1 on the phase-separated structure in the solvent cast films, we conducted time-resolved light scattering studies during the phase separation of the ternary polymer solutions. It may be needless to say that studies will provide valuable in-

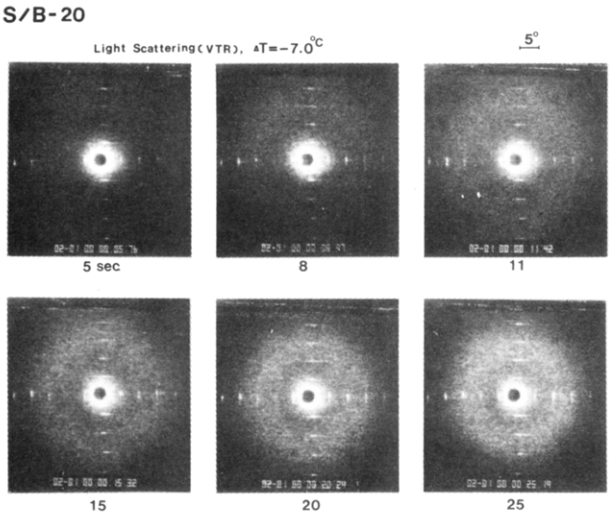

Figure 9. Evolution of light scattering pattern with time after inserting the sample cell, initially embedded in a medium at 50 °C, into the heated metal block controlled at phase-separation temperature T_x for S/B-20 with $\phi_0 = 0.905$ (volume fraction of toluene in the ternary mixture). The quench depth $\Delta T = T_x - T_{cl}$ was set at −7.0 °C where $T_{cl} = 43$ °C. Temperature of the sample cell reached to $T_x = \Delta T + T_{cl} = 36$ °C approximately 20 s after the insertion of the cell to the heated block. The number indicated under each pattern corresponds to the time after the insertion.

formation on the mechanism and kinetics of phase separation of the ternary system.

The ternary mixtures at fixed polymer concentrations ($1 - \phi_0 = 0.095$ for S/B-20 and $1 - \phi_0 = 0.115$ for S/SB-65) were enclosed in the cell, and isothermal phase-separation process were observed as a function of time after rapidly dropping temperature from T_i (=50 °C, higher than cloud points) to T_x (lower than the cloud points). For PS/PB/Tol, observations were made for off-critical mixture (i.e., $\theta_2 = 0.2$) and for near-critical mixture (i.e., $\theta_2 = 0.65$).

(a) Spinodal Decomposition. Figure 9 shows evolution of light scattering patterns during phase separation of the ternary mixture of S/B-20 ($\phi_0 = 0.905$) at quench depth $\Delta T = T_x - T_{cl} = -7.0$ °C (T_{cl} being the cloud point 43 °C, and T_x being the temperature that the cell attains in equilibrium and being equal to the temperature of the metal block) as observed by the silicone vidicon and VTR system. The figure includes the distance mark corresponding to $\theta = 5°$ and the time when each pattern was recorded. The time always refers to the time after insertion of the sample cell into the metal block, throughout the paper. As pointed out earlier, the initial temperature was always kept at 50 °C, above T_{cl}'s, and the temperature change was characterized by the relaxation time τ of 9.8 s. A further change of the scattering patterns after 25–120 s is shown in Figure 10.

From a quantitative analysis of kinetics of the phase separation as will be discussed in a forthcoming paper,[7] the spinodal temperature for this system S/B-20 was found to be 3 °C below the cloud point ($\Delta T_s = -3$ °C). The quench depth of $|\Delta T| = 7$ is greater than 3, and hence the phase separation should occur according to spinodal decomposition under this condition. From Figures 9 and 10 it is seen, qualitatively but clearly, that after several seconds the scattering maximum appears at $\theta = 14.4°$ and that the maximum intensity increases with time but peak position remains essentially unchanged up to about 40 s.

The above experimental evidence suggests that periodic concentration fluctuation of periodicity 2.5 μm starts to develop after the temperature drop and that this periodicity itself remains essentially unaltered but the amplitude

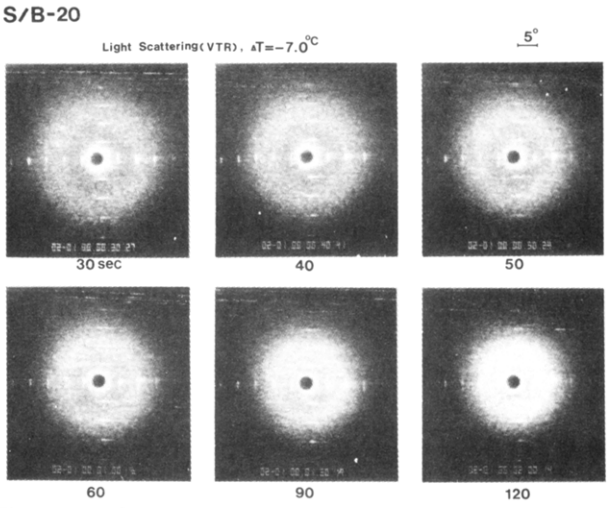

Figure 10. Change of the scattering pattern with time after 30 s. Other conditions are the same as those in Figure 9.

of the concentration fluctuation increases with time, in the initial stage of the phase separation, up to about 40 s. These results are in good agreement with the predictions given by Cahn's linearized theory of the spinodal decomposition.[2,24]

It may be noteworthy that our *ternary systems* can be treated as a *pseudobinary* system for which the theories developed for the binary systems can be applied with a good approximation. This is because toluene is a neutrally good solvent[8] for both polymers used in this work. Thus the phase separation of the ternary systems may be treated as that between PS solution and PB (or SB) solution, and the solvent essentially weakens the effective interaction between the two polymers.

As the phase separation further progresses, the maximum intensity further increases, and the peak position starts to sift toward small angles as seen in Figure 10, indicating that the periodicity of fluctuations as well as the amplitude of fluctuations further increase with time. It should be pointed out in Figure 10 that all the scattering patterns have the scattering maximum, although the maximum may be hard to observe, owing to an overexposure. The change of the scattering patterns 40 s after phase separation is relevant to the later stage of the spinodal decomposition where various coarsening processes occur.[10–18]

The evolution of the scattering patterns with time after the phase separation involved by the temperature drops for the ternary systems of S/SB-65 ($\phi_0 = 0.885$) at $\Delta T = -6.0$ °C is shown in Figures 11 and 12. The S/SB-65 system has composition near $\theta_{2,c}$ so that the system will undergo spinodal decomposition irrespective of the magnitude of the quench depth ΔT. Since one type of polymer is SB diblock polymer, one generally has to think microphase separation of SB as well as polymer solution–polymer solution phase separation of one's current interest here. The volume fraction of SB in the ternary system ϕ_{SB}, is equal to $(1 - \phi_0)\theta_2 = 0.125 \times 0.65 = 0.08$, the concentration of which is expected to be well below the critical concentration for the microphase separation of the SB block polymer.[19,20] Consequently, incorporation of the polystyrene block in SB does not complicate the polymer–polymer phase separation but essentially weakens the interaction between the constituent polymers.

The scattering maximum appears shortly after the onset of phase separation (less than 10 s). The maximum intensity increases with time but the peak position essentially remains unaltered up to about 30 s, having the periodicity

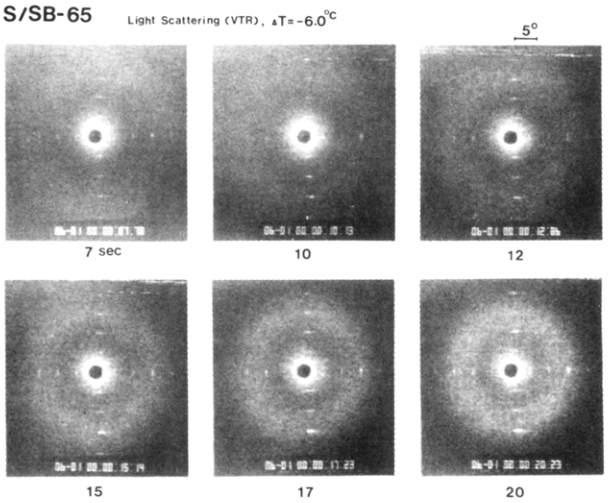

Figure 11. Evolution of the scattering pattern with time for S/SB-65 with $\phi_0 = 0.885$. The quench depth was set at −6 °C where $T_{cl} = 36$ °C ($T_x = 30$ °C). Other conditions are the same as in Figure 11.

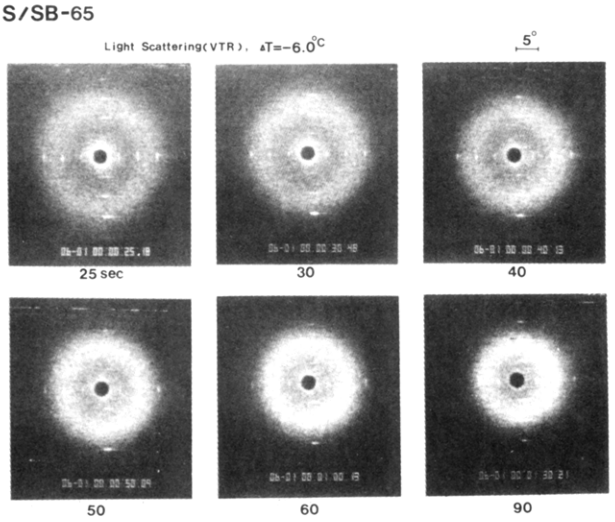

Figure 12. Change of the light scattering pattern with time after 25 s. Other conditions are the same as those in Figure 11.

of 2.6 μm. These results again are relevant to the early stage of spinodal decomposition as characterized by Cahn's linearized theory of spinodal decomposition.[2,24] As time goes on, the maximum scattering intensity further increases and peak positions start to shift toward smaller angles, corresponding again to a later stage of SD where various types of coalescence processes prevail.[10-18]

(b) Nucleation and Growth. Evolution of the scattering pattern during the nucleation and growth (NG) process was also investigated for the ternary system S/B-20, for the same system as studied in section III-3(a). The NG mechanism was found to occur for $|\Delta T| < |\Delta T_s| = 3$ °C by observing time evolution of the scattering as a function of quench depth, ΔT.[7]

Figure 13 shows the time evolution of scattering patterns after the phase separation at $\Delta T = -2$ °C. In contrast to the cases presented in the previous section, the scattering maximum was not observed during the entire time scale of the phase separation. At any time instances, the scattered intensity monotonically decreased with increasing θ, but the intensity level itself increases with time. This observation is believed to be typical of the case where the phase separation occurs according to the NG mechanism. The homogeneous and sporadic nucleation and growth of the domains will result in the broad distribution in the

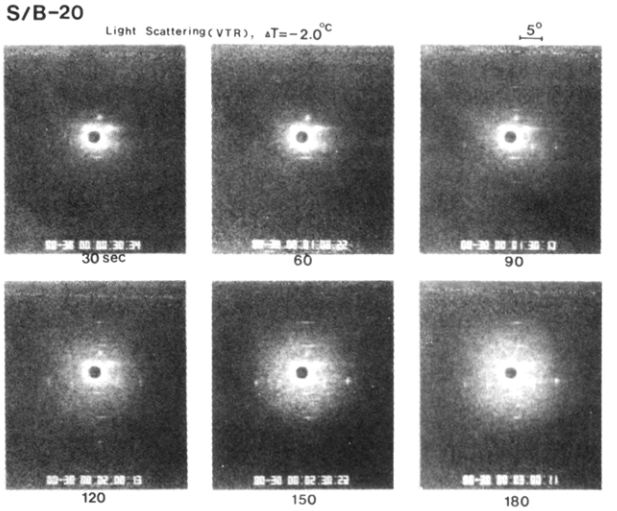

Figure 13. Evolution of light scattering pattern with time for S/B-20 in nucleation and growth regime. $\phi_0 = 0.905$, $\Delta T = -2.0$ °C ($T_x = 41$ °C and $T_{cl} = 43$ °C). (Other conditions are the same as in Figure 9.)

sizes of the dispersed domains, which would give rise to the observed monotonic scattering profiles with θ.

IV. Concluding Remarks

The mechanism and kinetics of phase separation were studied for ternary systems composed of polymer A, polymer B, and a neutrally good solvent for both polymers. The systems studied exhibit a phase diagram with UCST (upper critical solution temperature). Below UCST the systems undergo phase separation between polymer A solution and polymer B solution, the critical polymer compositions $(\theta_{2,c})_{obsd}$ and $(\theta_{1,c})_{obsd}$ being not predicted well by Scott's mean-field theory.[5]

The early stage of spinodal decomposition of the ternary systems was found to be describable by the linearized theory of Cahn.[2,24] For the quench depth studied in this paper ($|\Delta T| = 6$–7 °C) the time scale of this behavior was found to be typically less than 30–40 s, after which coarsening processes relevant to the later stage of spinodal decomposition prevail. The scattered intensity profiles evolved by the isothermal phase separation at a given polymer concentration are dramatically different, depending on mechansim of the phase separation (SD vs. NG). Thus the scattering method will provide a quick and sensitive way to distinguish the two mechanisms, at least for the ternary systems studied.

The phase-separated structures obtained in the solvent cast films are inevitably affected by the phase-separated structures developed and grown during the solvent evaporation, especially by the spinodal decomposition and subsequent coalescence processes. The structure developed in the solution is *kinetically frozen in* at some stage of spinodal decomposition, owing to increased time required for equilibration at high concentrations, resulting in the structure in the solid films. The final solid structure is then controlled by a competition of the two rate constants, i.e., growth rate of phase separation (especially spinodal decomposition) and evaporation rate of solvent. The relative importance of spinodal vs. coalescence processes in the film formation should generally depend on the competition of the two rate constants, but qualitatively the latter process seems to dominate. The prediction of the final structure is not still simple, owing to the fact that one has to deal with *athermal growth* of spinodal decomposition. The key to understanding the final structure would seem to be the cumulative information on the iso-

thermal processes, as partially described in this paper.

Acknowledgment. This work is partially supported by a Grant-in-Aid for Special Project Research (No. 57119003) from the Ministry of Education, Science and Culture of Japan ("Design of Multiphase Biomedical Materials") and by scientific grants from the Asahi Glass Foundation for Industrial Technology, Toyoda Gosei Co., Ltd., and the Yokohama Rubber Co., Ltd.

References and Notes

(1) Hashimoto, T.; Kumaki, J.; Kawai, H. *Macromolecules* **1983**, 16, 641.
(2) Cahn, J. W. *J. Chem. Phys.* **1965**, *42*, 93.
(3) Dupplessix, R.; Picot, C.; Benoit, H. *J. Polym., Sci., Polym. Lett. Ed.* **1971**, *9*, 321.
(4) Flory, P. J. "Principles of Polymer Chemistry"; Cornell University Press: Ithaca, NY, 1967.
(5) Scott, R. L. *J. Chem. Phys.* **1949**, *17*, 268.
(6) Tompa, H. "Polymer Solutions"; Butterworths: London, 1956.
(7) Part 3: Sasaki, K.; Hashimoto, T. *Macromolecules*, following paper in this issue.
(8) χ values for the interaction of PS-Tol, PB-Tol, and PS-PB are 0.436, 0.465, and 0.10, respectively, according to Noolandi and Hong.[9]
(9) Noolandi, J.; Hong, K. M. *Ferroelectrics* **1980**, *30*, 117.
(10) Langer, J. S.; Bar-on, M.; Miller, H. D. *Phys. Rev. A* **1975**, *11*, 1417.
(11) Binder, K.; Stauffer, D. *Phys. Rev. Lett.* **1974**, *33*, 1006.
(12) Kawasaki, K.; Ohta, T. *Prog. Theor. Phys.* **1978**, *59*, 362.
(13) Lifshitz, I. M.; Slyozov, V. V. *J. Phys. Chem. Solids* **1961**, *19*, 35.
(14) Siggia, E. D. *Phys. Rev. A* **1979**, *20*, 595.
(15) Nojima, S.; Tsutsumi, K.; Nose, T. *Polym. J.* **1982**, *14*, 225.
(16) Kuwahara, N.; Tachikawa, M.; Hamano, K.; Kenmochi, Y. *Phys. Rev. A* **1982**, *25*, 3349.
(17) Snyder, H. L.; Meakin, P.; Reich, S. *J. Chem. Phys.* **1983**, *78* (6), 3334.
(18) Shimidzu, N.; Hashimoto, T.; Kawai, H., to be submitted to *Macromolecules* (part 4 of this series).
(19) Hashimoto, T.; Shibayama, M.; Kawai, H. *Macromolecules* **1983**, *16*, 1093.
(20) Shibayama, M.; Hashimoto, T.; Hasegawa, H.; Kawai, H. *Macromolecules* **1983**, *16*, 1427.
(21) Van Aartsen, J. J. *Eur. Polym. J.* **1970**, *6*, 919.
(22) Van Aartsen, J. J.; Smolders, C. A. *Eur. Polym. J.* **1970**, *6*, 1105.
(23) Feke, T.; Prins, W. *Macromolecules* **1974**, *7*, 527.
(24) The results presented here are consistent with the Cahn model but are also consistent with the Cook model,[25] a sort of modified Cahn model. The results may also be consistent qualitatively with Langer's model,[10] since in Langer's prediction the scattering maximum is only slowly varying.
(25) Cook, H. E. *Acta Metall.* **1970**, *18*, 297.
(26) Nish, T.; Wang, T. T.; Kwei, T. K. *Macromolecules* **1975**, *8*, 227.
(27) Snyder, H. L.; Meakin, P.; Reich, S. *Macromolecules* **1983**, *16*, 757.
(28) Gelles, R.; Frank, C. W. *Macromolecules* **1983**, *16*, 1448.
(29) It should be noted that eq 1 is valid for isolated spheres with monodisperse size distribution. In the case when the polydispersity exists in the size, eq 1 is only qualitatively true, and the rigorous value of $4\pi (R_s/\lambda) \sin (\theta_m/2)$ (R_s, average radius) depends on the distribution function for the particle size.
(30) One should note that the arguments similar to those in ref 29 must be applied on distribution of the periodicity D_s. The average periodicity D_s in real space will give only a qualitatively correct peak position in reciprocal space.

Time-Resolved Light Scattering Studies on the Kinetics of Phase Separation and Phase Dissolution of Polymer Blends. 3. Spinodal Decomposition of Ternary Mixtures of Polymer A, Polymer B, and Solvent

Kouji Sasaki† and Takeji Hashimoto*

Department of Polymer Chemistry, Faculty of Engineering, Kyoto University, Kyoto 606, Japan. *Received January 4, 1984*

ABSTRACT: An early stage of spinodal decomposition (SD) for the ternary mixtures of polystyrene (PS), polybutadiene (PB), and toluene (Tol) and of PS, polystyrene–polybutadiene diblock polymer (SB), and Tol was investigated by the time-resolved light scattering technique. The SD for the ternary systems in which Tol is a neutrally good solvent for all the polymers used in these studies was analyzed on the basis of the linearized theory of Cahn, coupled with a pseudobinary approximation and a mean-field approximation for the ternary solutions. An overall behavior in the early stage of SD seems to fit well, at least qualitatively, with the linearized theory coupled with the above two approximations. Quantitative deviations from the theory were observed, and they may be attributed to the validity of the special (mean field) model used for the ternary solutions and/or of the linearized theory, besides the experimental errors arising from difficulties studying the earliest stage of the process. The characteristic parameters describing the early stage of SD for the ternary systems were obtained in the context of the linearized theory and compared with those for the binary mixture of PS and poly(vinyl methyl ether).

I. Introduction

In the previous paper,[1] we found a spatial composition fluctuation with a characteristic periodicity which gives rise to a light scattering maximum for the films composed of binary and ternary mixtures of polystyrene (PS), polybutadiene (PB), and polystyrene–polybutadiene diblock polymers (SB) prepared by solvent casting with toluene (Tol), a neutrally good solvent for these polymers. These periodic fluctuations are found to develop and grow in the solutions during the phase separation due to spinodal decomposition (SD) and its subsequent coalescence processes.[2-14] The existence of SD and the coalescence processes were qualitatively demonstrated by a time-resolved laser light scattering technique using a silicone vidicon TV camera and VTR monitor system for the ternary systems composed of PS, PB, and Tol or PS, SB, and Tol.[1]

In the present paper we will focus our attention on the very early stage of SD for the ternary systems composed of PS/PB/Tol and PS/SB/Tol at critical and off-critical compositions. Section II describes the time-resolved light

†Present address: Toyoda Gosei Co., Ltd., 1, Nagahata, Ochiai, Haruhi-Mura, Nishikasugai-gun, Aichi-Prefecture 452, Japan.

0024-9297/84/2217-2818$01.50/0